Steel and Composite Structures, Vol. 6, No. 6 (2006) 459-477
DOI: http://dx.doi.org/10.12989/scs.2006.6.6.459

Integrated analysis and design of composite beams with flexible shear connectors under sagging and hogging moments

A. J. Wang† and K. F. Chung‡

Department of Civil and Structural Engineering, The Hong Kong Polytechnic University, Hong Kong SAR, China

(Received August 18, 2005, Accepted January 3, 2006)

Abstract. A theoretical research project is undertaken to develop integrated analysis and design tools for long span composite beams in modern high-rise buildings, and it aims to develop non-linear finite element models for practical design of composite beams. As the first paper in the series, this paper presents the development study as well as the calibration exercise of the proposed finite element models for simply supported composite beams. Other practical issues such as continuous composite beams, the provision of web openings for passage of building services, the partial continuity offered by the connections to columns as well as the behaviour of both unprotected and protected composite beams under fires will be reported separately. In this paper, details of the finite elements and the material models for both steel and reinforced concrete are first described, and finite element studies of composite beams with full details of test data are then presented. It should be noted that in the proposed finite element models, both steel beams and concrete slabs are modelled with two dimensional plane stress elements whose widths are assigned to be equal to the widths of concrete flanges, and the flange widths and the web thicknesses of steel beams as appropriate. Moreover, each shear connector is modelled with one horizontal spring and one vertical spring to simulate its longitudinal shear and pull-out actions based on measured load-slippage curves of push-out tests of shear connectors. The numerical results are then carefully analyzed and compared with the corresponding test results in terms of load mid-span deflection curves as well as load end-slippage curves. Other deformation characteristics of the composite beams such as stress and strain distributions across the composite cross-sections as well as distributions of shear forces and slippages in shear connectors along the beam spans are also examined in details. It is shown that the numerical results of the composite beams compare well with the test data in terms of various load-deformation characteristics along the entire deformation ranges. Hence, the proposed analysis and design tools are considered to be simple and yet effective for composite beams with practical geometrical dimensions and arrangements. Structural engineers are strongly encouraged to employ the models in their practical work to exploit the full advantages offered by composite construction.

Keywords: composite beams; finite element models; integrated analysis and design; bending; shear; degree of shear connection.

1. Practical design of composite beams

In modern structural design codes of composite structures, plastic analysis principles are adopted in designing composite beams, and their moment resistances under sagging and hogging moments are

†Research Student
‡Professor, Corresponding author, E-mail: cekchung@polyu.edu.hk

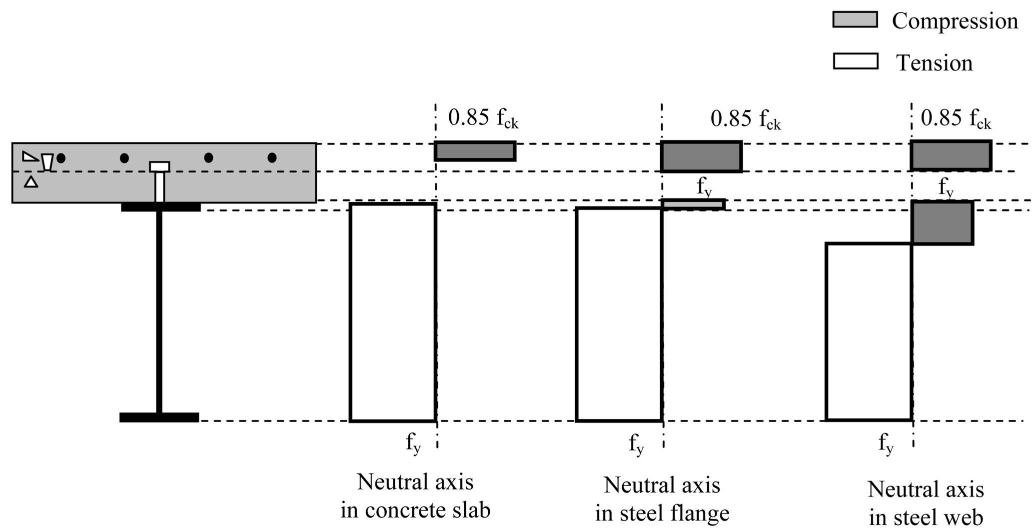

(a) Composite beams under sagging moment

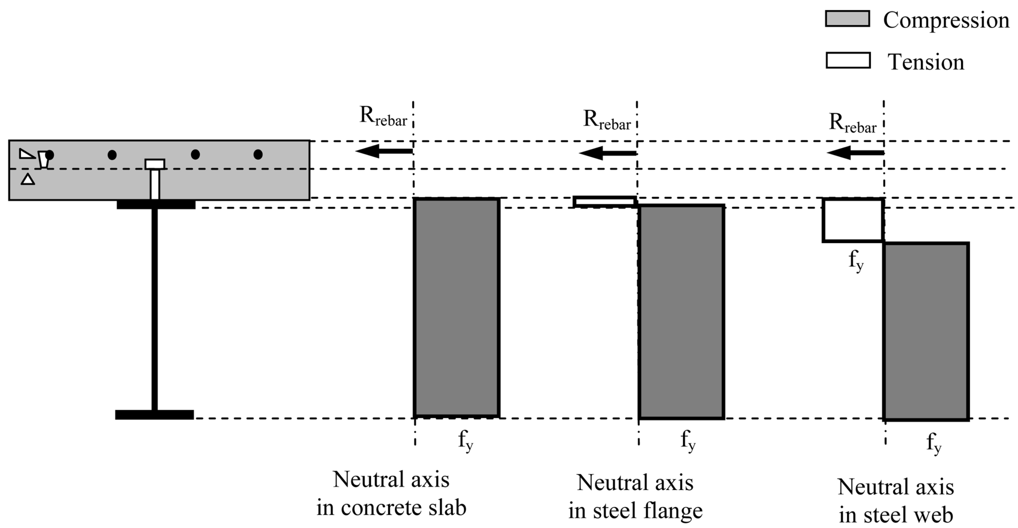

(b) Composite beams under hogging moment

Fig. 1 Plastic stress blocks of composite beams

determined using plastic stress blocks, as shown in Fig. 1. Depending on the relative strength and ductility of shear connectors at the interface between the concrete slab and the steel section, the deformation characteristic of a composite beam varies considerably. At present, simplified design methods for composite beams with full or partial shear connection are given in various design codes such as BS5950 (1990), AS2327 (1996), Eurocode 4 (2002), and Hong Kong Steel Code (2005) while design handbooks for composite beams with either solid concrete slabs or composite slabs with profiled steel decking (Lawson 1989, Johnson and Anderson 2001, Lawson and Chung 1994, Oehlers and Bradford 1995, AS2327.1 1997) may also be found.

In general, reference to specialist design guides is often needed for structural engineers in designing composite beams and floor systems with practical constructional features such as composite beams with asymmetric I sections or fabricated I sections with tapered webs, perforated composite beams for full integration with building services, composite beams with partial continuity offered by the connections with columns, and long span composite beams against vibration. At present, many design methods and procedures are available in the literature, but most of them are code-specific and iterations are often required to achieve high structural economy. In general, it is found that their uses in practice are fairly limited as structural engineers cannot afford the time to learn each design procedure, and then perform each design separately. Moreover, there are practical cases which are not covered by any of these design methods. Hence, it is highly desirable to develop integrated analysis and design tools for practical design of composite beams.

1.1. Advanced analytical and numerical models

In order to predict accurately and design adequately the structural behaviour of composite beams with flexible shear connectors, several attempts with different analytical and numerical models are found in the literature. Simplified analytical models based on classical moment curvature methods modified with the presence of slippages due to flexible shear connectors at the interfaces between concrete slabs and steel beams are reported (Oehlers and Sved 1995, Wang 1998). It is shown that deformation characteristics of composite beams with very low degrees of shear connection are predicted satisfactorily when compared with test results.

A number of finite element studies on the general behaviour of composite beams with flexible shear connectors are also reported by Gattresco (1999), Hassan and Mourad (2002), Baskar *et al*. (2002), and Cas *et al*. (2004). In these studies, the composite beams are represented by two or three dimensional models, and the concrete slabs and the steel beams are modelled with different elements such as beam-column elements, plane stress elements, shell elements, or even solid elements while the shear connectors are modelled with spring or beam elements. With the carefully selected stress-strain curves for both reinforced concrete slabs and steel beams as well as the nonlinear load-slippage curves of shear connectors, it is demonstrated that these finite element models are able to predict satisfactorily the structural behaviour of composite beams under simply or continuously supported conditions. However, these studies mainly concern composite beams under sagging moments with moderate to high degrees of shear connection, and the computational efforts are considerable.

An advanced numerical study on composite frames with partial shear connection (Fang *et al*. 2000) is reported in the literature where discrete shear connectors are assumed to be continuous along the interfaces between the concrete slabs and the steel beams. Hence, an entire composite beam is modelled as a single beam-column element with a hybrid mixed-shape function for transverse deformations which is superior to the commonly used polynomial displacement functions. Moreover, an advanced numerical model using three dimensional elements is established (Lam and El-Lobody 2005) to examine the structural behaviour of headed shear connectors in composite beam construction. The models are shown to be effective in simulating the load-slippage curves of headed shear studs in solid reinforced concrete slabs in push-out tests, and hence, it provides detailed information to the different modes of failure observed in tests.

1.2. Investigation on composite beams under hogging moments

An extensive investigation on the effects of partial shear connection in the hogging moment regions of composite beams is reported by Loh *et al*. (2004a,b) where a total of eight composite beams are tested under static and repeated cyclic loadings. The main parameters under investigation include the degree of shear connection, the steel reinforcement ratios, and the effects of repeated loading. In addition, three complementary push-out tests are also conducted to obtain the load-slippage curves of the shear connectors. It is found that all the composite beams with partial shear connection under hogging moment perform satisfactorily in terms of strength and ductility. Furthermore, an iterative-based analytical model is proposed to examine the structural behaviour of composite beams under hogging moments with partial shear connection; slippage at the interfaces between concrete flanges and steel beams is incorporated with full compliance to equilibrium and compatibility requirements. The analysis results show that reasonable agreement with the results of the eight composite beams is achieved, and the flexural response of the beams including slippage of shear connectors is predicted adequately until failure.

2. Objectives and scope of work

A theoretical research project is undertaken by the authors to develop integrated analysis and design tools for long span composite beams in modern high-rise buildings, and it aims to develop non-linear finite element models for practical design of composite beams (Chung and Wang 2004, Chung *et al*. 2005). As the first paper in the series, this paper presents the development study as well as the calibration exercise of the proposed finite element models for simply supported composite beams. Other practical issues such as continuous composite beams, the provision of web openings for passage of building services, the partial continuity offered by the connections to columns as well as the behaviour of unprotected and protected composite beams under fires will be reported separately.

In this paper, details of the finite elements and the material models for both steel and concrete are first described, and finite element studies of composite beams with full details of test data (Loh *et al*. 2004a, Jayas and Hosain 1989, McGarraugh and Baldwin 1971) reported in the literature are then presented. The numerical results are carefully analyzed and compared with the corresponding test results in terms of load mid-span deflection curves and load end-slippage curves. Other deformation characteristics of the composite beams such as stress and strain distributions across the composite cross-sections as well as distributions of shear forces and slippages in shear connectors along the beam spans are also examined in details.

In order to ensure the general applicability of the proposed finite element models, six composite beams with fully documented test results (Loh *et al*. 2004a, Jayas and Hosain 1989, McGarraugh and Baldwin 1971) covering a wide range of practical parameters are selected from the literature for the calibration of the finite element models. Hence, the proposed models are applicable to composite beams with the following features:

- normal strength concrete with steel beams of both mild steel and high strength steel,
- concrete solid slabs, and composite slabs with profiled steel decking,
- long to short beam spans with wide to narrow concrete flanges,
- one or two shear connectors per row with various degrees of shear connection at critical cross-sections, and
- flexural failure under sagging and hogging moments in long span beams, and also section failure under combined bending and shear in short span beams.

Table 1 presents the general information of the composite beam tests while the measured yield strengths of steel beams and the measured cylinder strengths of concrete are summarized in Table 2 together with

Table 1 Summary of composite beam tests

Researchers	Year	Beam test	Type of moment	Type of concrete slab	Span, L (mm)	Depth of steel section, D(mm)	Depth of composite section, D_c(mm)	L/D_c	Nominal width of concrete slab B_s(mm)	Effective width of concrete slab B_e(mm)	B_s/L
McGarraugh and Baldwin	1971	B2	Sagging	Solid	6705	352	466	14	914	914	0.14
		B4	Sagging	Solid	6705	352	466	14	1829	1676	0.27
Jayas and Hosain	1989	JP1	Sagging	Composite	4100	317	469	8.7	1220	1025	0.30
		JP2	Sagging	Composite	2050	317	469	4.4	1220	513	0.60
Loh, Uy and Bradford	2004	CB2	Hogging	Composite	2500	248	368	6.7	515	625	0.21
		CB3	Hogging	Composite	2500	248	368	6.7	515	625	0.21

Table 2 Measured strengths of composite beams

Beam test	Measured yield strength of steel, p_y (N/mm^2)	Measured cylinder strength of concrete, p_c (N/mm^2)	Measured yield strength of reinforcement, $p_{y,r}$ (N/mm^2)	Measured yield strength of profiled steel decking, $p_{y,d}$ (N/mm^2)
B2	252.5	38.4	-	-
B4	244.3	33.8	-	-
JP1	341.0	26.9	337	-
JP2	341.0	30.4	342	-
CB2	400.0	26.9	500	600
CB3	400.0	26.9	500	600

the nominal yield strengths of both reinforcement and profiled steel deckings, whenever available. The general layouts of the test set-ups together with the geometrical dimensions of the composite beams as well as the arrangements of shear connectors are fully illustrated in Figs. 2, 3 and 4 for easy reference.

It should be noted that in all these six composite beam tests, complementary push-out tests of the shear connectors are carried out by the investigators and fully reported in the literature, and they provide important deformation characteristics of the shear connectors in the finite element models.

3. Finite element modelling

In order to simulate numerically the structural behaviour of composite beams under practical loading and support conditions, a finite element model is established using the general purpose finite element package ABAQUS (Version 6.4, 2004). It should be noted that since the principal failure modes in composite beams involve only in-plane deformation while out-of-plane instability is effectively prohibited in practice, two-dimensional finite element models are adopted for simplicity. Moreover, iso-parametric four-node two-dimensional plane stress elements, CPS4R, are used to model the concrete slabs and the steel beams, as well as the profiled steel decking as appropriate. Hence, there are two translational displacements and one rotation at each node of the plane stress elements while two in-plane direct stresses and one in-plane shear stress are incorporated in each side of the elements.

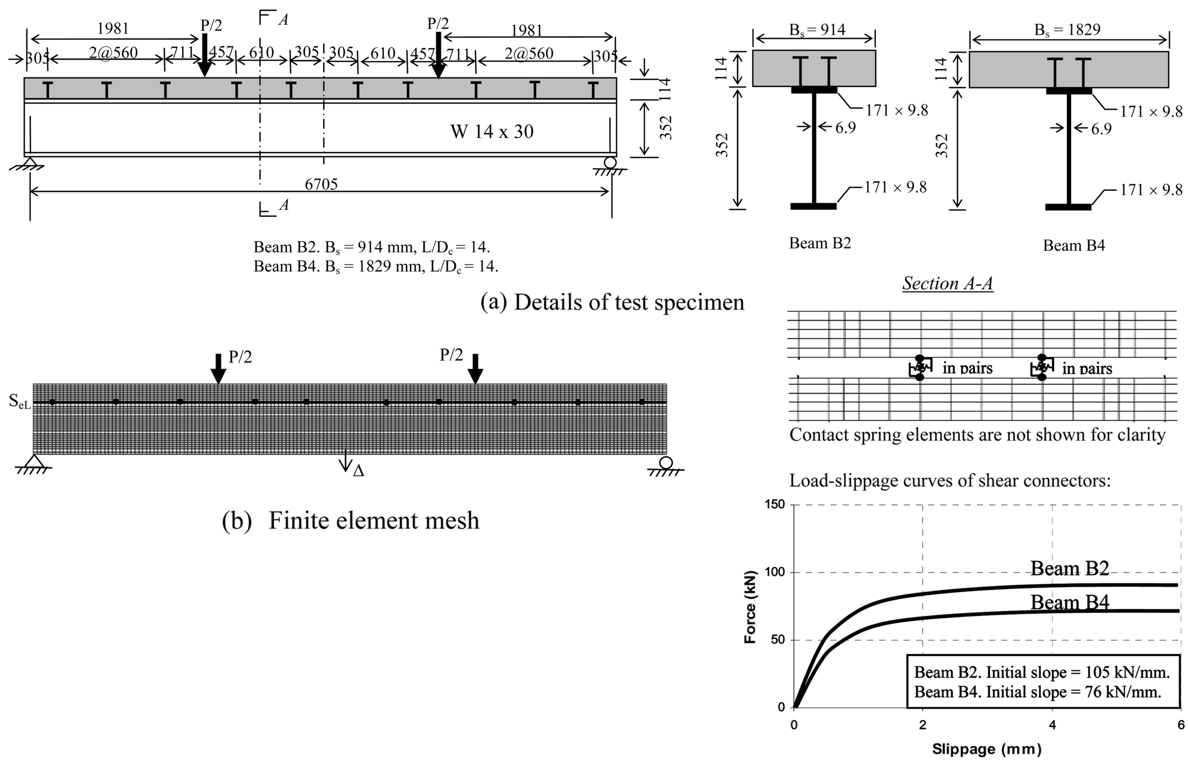

Fig. 2 Beams B2 and B4

3.1. Material models

For the material model of steel, a bi-linear stress-strain curve shown in Fig. 5(a) is adopted.

For concrete under uni-axial loading condition, a non-linear stress-strain curve as shown in Fig. 5(b) is adopted in the material model. The compressive strength of concrete is taken to be its cylinder strength while its tensile strength is taken as only 10% of its compressive value. The limiting compressive strain of concrete against crushing is taken to be 0.35%. In order to simulate micro-cracks in concrete under tension, the concept of 'smeared cracking' is adopted where the tensile strength of concrete is assumed to be reduced linearly to zero at a tensile strain of 0.1% at which all the micro-cracks are fully open.

Moreover, the Drucker-Prager failure criterion (Baskar *et al.* 2002) is adopted for concrete under bi-axial loading condition as follows:

$$q - p \tan \beta - c \leq 0 \tag{1}$$

where

q is the Mises equivalent stress;

$$= \frac{1}{\sqrt{2}} \sqrt{(\sigma_2 - \sigma_2)^2 + \sigma_1^2 + \sigma_2^2}$$

σ_1 and σ_2 are the maximum and the minimum principle stresses respectively;

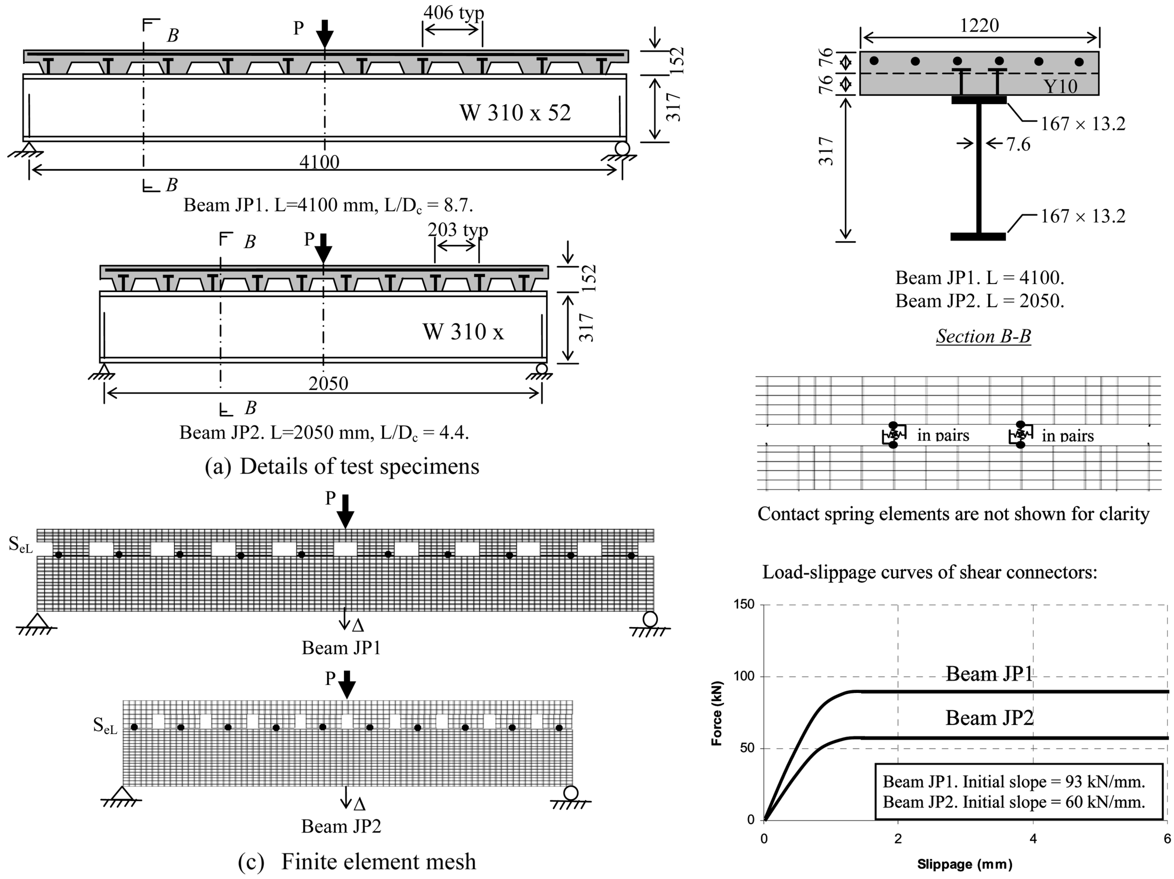

Fig. 3 Beams JP1 and JP2

p is the equivalent pressure stress; $= \dfrac{\sigma_1 + \sigma_2}{2}$;

β is the friction angle of concrete; = 67.5° for concrete with f_t / f_c=0.1 according to ABAQUS (2004);

c is the cohesion of concrete.

The corresponding failure surface is illustrated in Fig. 5(b).

While transverse reinforcement and profiled steel deckings are ignored in the models, both longitudinal reinforcement and profiled steel deckings are modelled through the use of 'smeared layers' together with a number of steel layers as well as concrete layers as shown in Fig. 6. The mechanical properties of the smeared layers, namely, the equivalent compressive strength, the equivalent tensile strength and the equivalent Young's modulus, are evaluated (Baskar *et al*. 2002) according to the areas and the material curves of concrete, reinforcement and profiled steel deckings as shown in Fig. 6. Typical transformation of a smear reinforced concrete layer in a composite slab with a corresponding bulk material curve is shown in Fig. 7. It should be noted that the adoption of smeared layers with corresponding bulk material curves allows the effect of concrete cracking to be accurately incorporated into the finite element models once the tensile strain of the smeared layers exceed the limiting tensile strain of concrete at 0.1%. Similarly, the effect of concrete crushing is also accurately incorporated into the finite

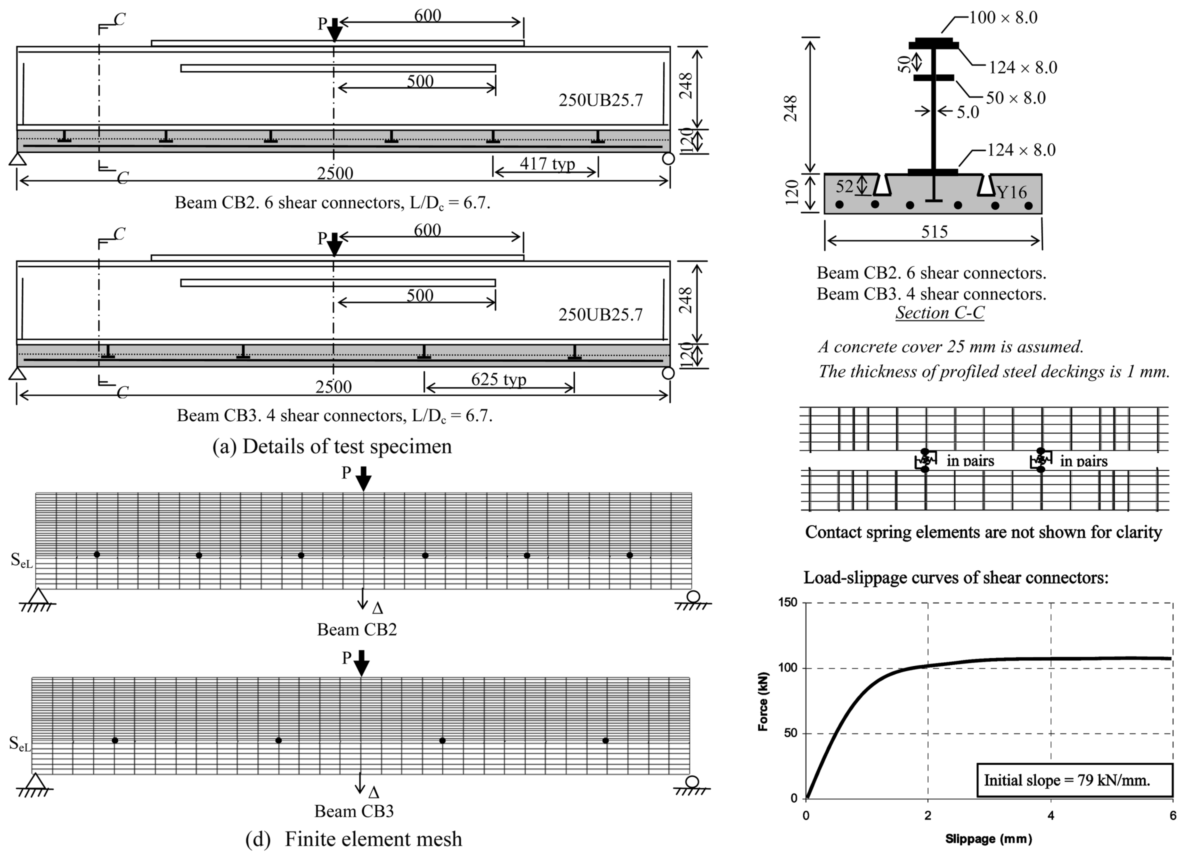

Fig. 4 Beams CB2 and CB3

element models once the compressive strain of the smeared layers exceeds the limiting compressive strain of concrete at 0.35%. Hence, a continuous bulk material curve of the smeared reinforced concrete layer which possesses significant ductility under both compression and tension is obtained as shown in Fig. 7, despite of severe discontinuities in the material curve of concrete. It is important to note that the presence of a smeared reinforced concrete layer among a number of concrete layers in composite beams and slabs is found to be very effective in suppressing numerical divergence during solution iterations, provided that practical configurations of reinforced concrete slabs as well as of composite slabs with profiled steel deckings are adopted.

Both smeared reinforced concrete layers and smeared composite decking layers are provided in the finite element models of Beams JP1, JP2, CB2 and CB3. However, no smeared reinforced concrete layers are provided in the finite element models of Beams B2 and B4 as no details of the reinforcement is found in the literature. Nevertheless, the errors in the finite element results are considered to be insignificant as shown in Beams JP1 and JP2 as the areas of the compression reinforcement are very small in comparison with those of the concrete in compression.

3.2. Two dimensional finite element models

With both material and geometric non-linearities incorporated into the finite element models, large

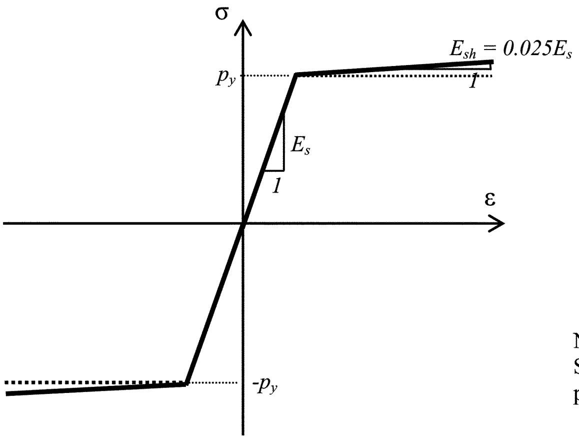

Note:
Similar stress-strain curves for reinforcement and profiled steel deckings.

(a) Steel

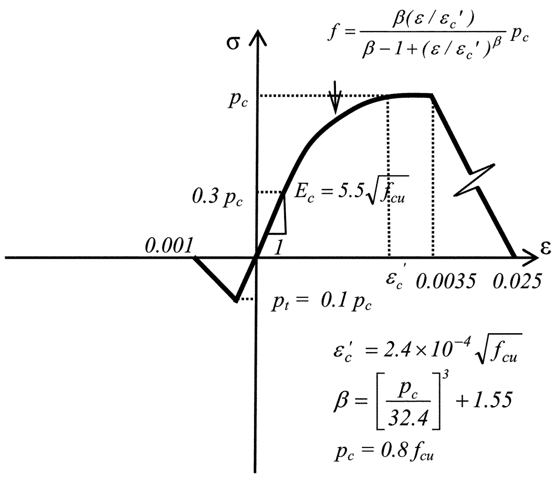

i. Uni-axial loading

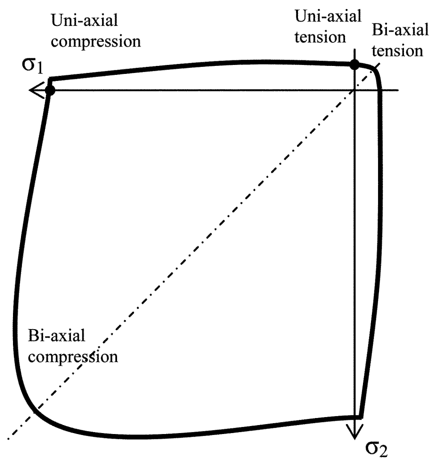

ii. Bi-axial loading

Beam test	Cohesion of concrete, c (N/mm^2)
B2	7.7
B4	6.8
JP1	5.4
JP2	6.1
CB2	5.4
CB3	5.4

(b) Concrete

Fig. 5 Material models

deformation in the critical section after steel yielding can be predicted accurately. Moreover, according to the geometry of the composite beams, the thicknesses of the plane stress elements are assigned to be equal to the widths of the concrete flanges as well as the flange widths and the web thicknesses of the

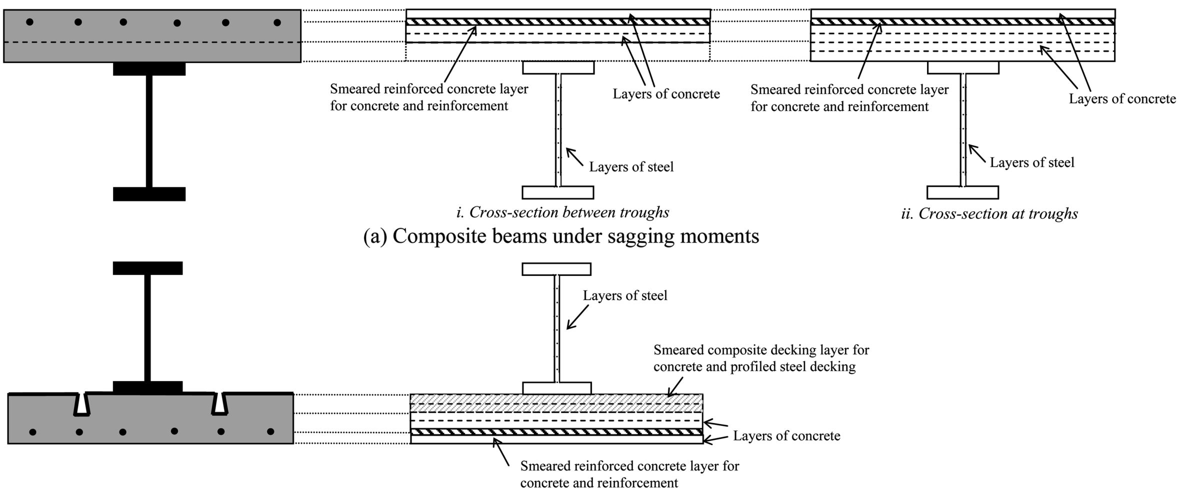

(b) Composite beams under hogging moments

$\sigma_s(\varepsilon_i)$	is the strength of reinforcement or profiled steel deckings at a strain of ε_i according to the material curves;
$\sigma_c(\varepsilon_i)$ and $\sigma_t(\varepsilon_i)$	are the compressive and the tensile strengths of concrete at a strain of ε_i according to the material curves;
A_s	is the area of reinforcement or profiled steel deckings in the smeared layer;
A_c	is the area of concrete in the smeared layer;
$E_s(\varepsilon_i)$	is the Young's modulus of reinforcement or profiled steel deckings at a strain of ε_i according to the material curves; and
$E_c(\varepsilon_i)$	is the Young's modulus of concrete at a strain of ε_i according to the material curves.

Equivalent compressive strength of the smeared layer:

$$\sigma_{eq,c}(\varepsilon_i) = \frac{\sigma_s(\varepsilon_i)\times A_s + \sigma_c(\varepsilon_i)\times A_c}{A_s + A_c}$$

Equivalent tensile strength of the smeared layer:

$$\sigma_{eq,t}(\varepsilon_i) = \frac{\sigma_s(\varepsilon_i)\times A_s + \sigma_t(\varepsilon_i)\times A_c}{A_s + A_c}$$

Equivalent Young's modulus of the smeared layer:

$$E_{eq}(\varepsilon_i) = \frac{E_s(\varepsilon_i)\times A_s + E_c(\varepsilon_i)\times A_c}{A_s + A_c}$$

Fig. 6 Smeared layers of reinforced concrete and composite deckings

steel beams as appropriate. The widths of the concrete flanges in the composite beams are taken as either the nominal widths or the effective widths, i.e., span/4, of the test beams, whichever is smaller. Both the nominal widths and the effective widths of the test beams are given in Table 1 for easy reference.

It should be noted that in order to simplify the finite element model, each shear connector is modelled with a horizontal spring element and a vertical spring element to simulate its longitudinal shear and pull-out actions respectively. In general, the deformation characteristics of the spring elements are obtained from push-out tests of shear connectors. Alternatively, idealised bi-linear curves may be adopted according to design values as appropriate. In the present study, the load slippage curves of shear connectors obtained from complementary push-out tests are adopted to be the deformation characteristics of the horizontal spring elements in the finite element models. Furthermore, the deformation characteristics of the vertical spring elements are taken to be similar to those of the horizontal spring elements for simplicity with the same stiffness but half of the strength.

The finite element models of the test beams are presented in Figs. 2, 3 and 4, illustrating the meshes of the models as well as the locations of the spring elements. In order to avoid local inclusion between the meshes of the concrete slabs and the steel beams during deformation, axial spring elements with extremely high compressive stiffnesses but zero tensile stiffness, or contact spring elements, are provided at the interfaces between the concrete slabs and the steel beams.

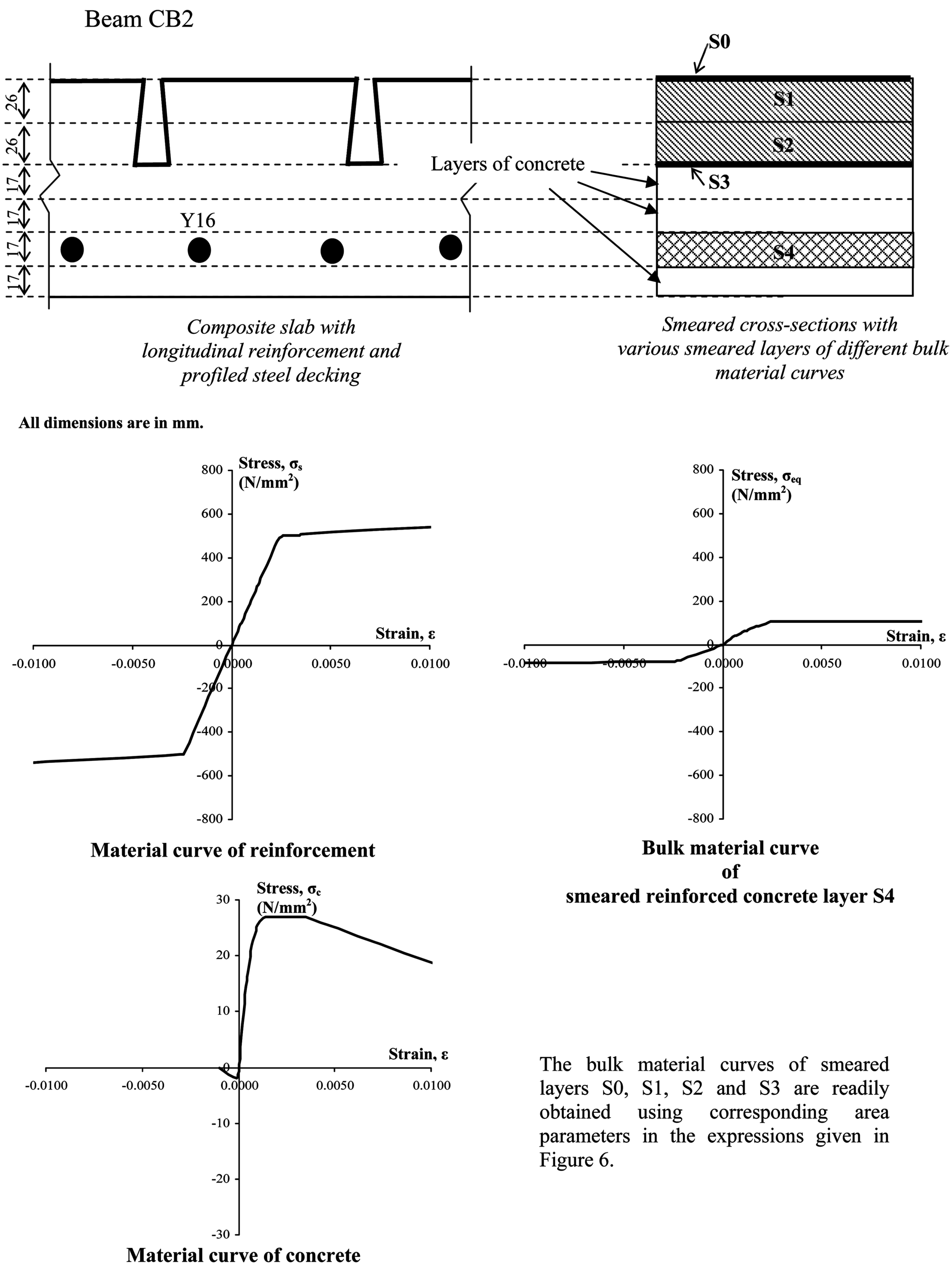

Fig. 7 Typical transformation of a smeared layer with a bulk material curve

4. Numerical studies and results

Due to the high efficiency of the finite element models, the computational efforts of all the models are found to be minimal, and numerical results are readily analyzed for rational interpretation. The following data of the six composite beams are fully presented in Figs. 8, 9 and 10:

- Load mid-span deflection curves,
- Load end-slippage curves,
- Stress and strain distributions across the depth of composite cross-sections, and
- Distributions of shear forces and slippages in shear connectors along the beam spans.

Comparison between the numerical and the test results is made whenever possible, and both numerical and test data are plotted onto the same graphs for direct comparison.

4.1. Load deflection curves

It is shown in Figs. 8, 9 and 10 that the load mid-span deflection curves obtained from the proposed finite element models of all the six composite beams follow closely to those measured data not only in the elastic deformation ranges but also in the large deformation ranges. Moreover, both the predicted and the measured load end-slippages curves of Tests CB2 and CB3 are also found to be very close to one another.

4.2. Ultimate loads

Table 3 summarizes both the measured values, P_{Test}, and the predicted values, P_{FEM}, of the ultimate loads of the composite beams. The shear force ratios are calculated according to the plastic shear resistances of the steel beams, i.e., shear area times plastic shear strength, while the shear areas of the steel beams include both the webs and the reinforcement plates in the webs, whenever applicable. It should be noted that only Beam JP2 fails in bending under high shear while all the other composite beams fail in flexure under sagging or hogging moments.

For back analysis purpose, the predicted ultimate loads of the composite beams are taken to be equal to the applied loads at large deformation where the maximum strain at any cross-section of the composite beams reaches the limiting value, ε_{max}, which is defined as follows:

$$\varepsilon_{max} = 6 \times \frac{p_y}{E_s}\sqrt{\frac{p_y}{275}} \tag{2}$$

where p_y is the measured yield strength of the steel section; and
E_s is the measured Young's modulus, and it may be taken as 205 kN/mm^2 in the absence of test data.

This limiting strain criterion is considered to be more rational than a limiting deflection criterion as it is independent on the geometrical configuration of composite beams, and equally applicable to composite beams under different support conditions. It is shown that based on the limiting strains defined in Eq. (2) above, the predicted ultimate loads of the composite beams are always conservative as well as close to the measured ones; the average value of the ratios P_{Test}/P_{FEM} in Table 3 is found to be 1.06.

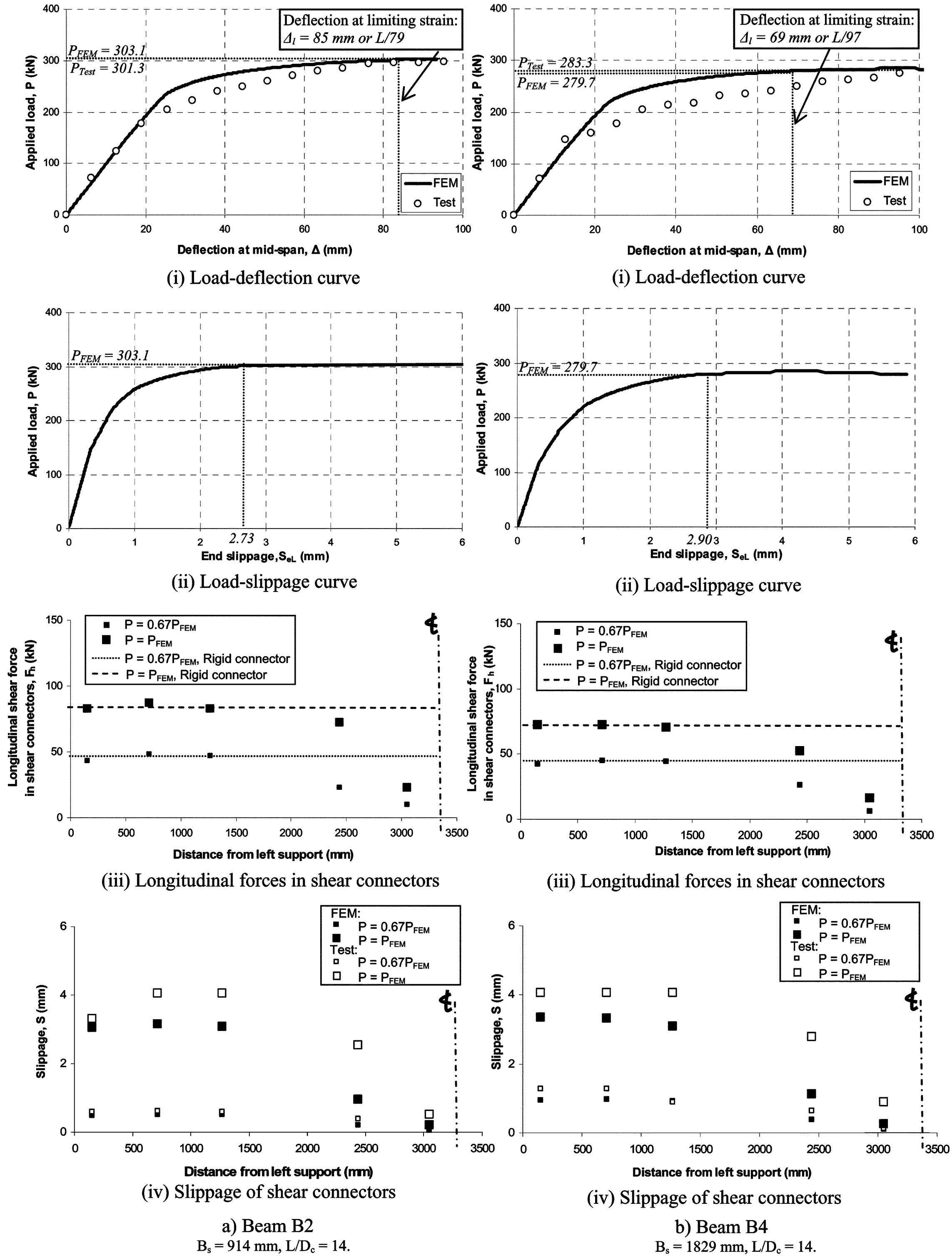

(i) Load-deflection curve

(ii) Load-slippage curve

(iii) Longitudinal forces in shear connectors

(iv) Slippage of shear connectors

a) Beam B2
B_s = 914 mm, L/D_c = 14.

b) Beam B4
B_s = 1829 mm, L/D_c = 14.

Fig. 8 Numerical results of Beams B2 and B4

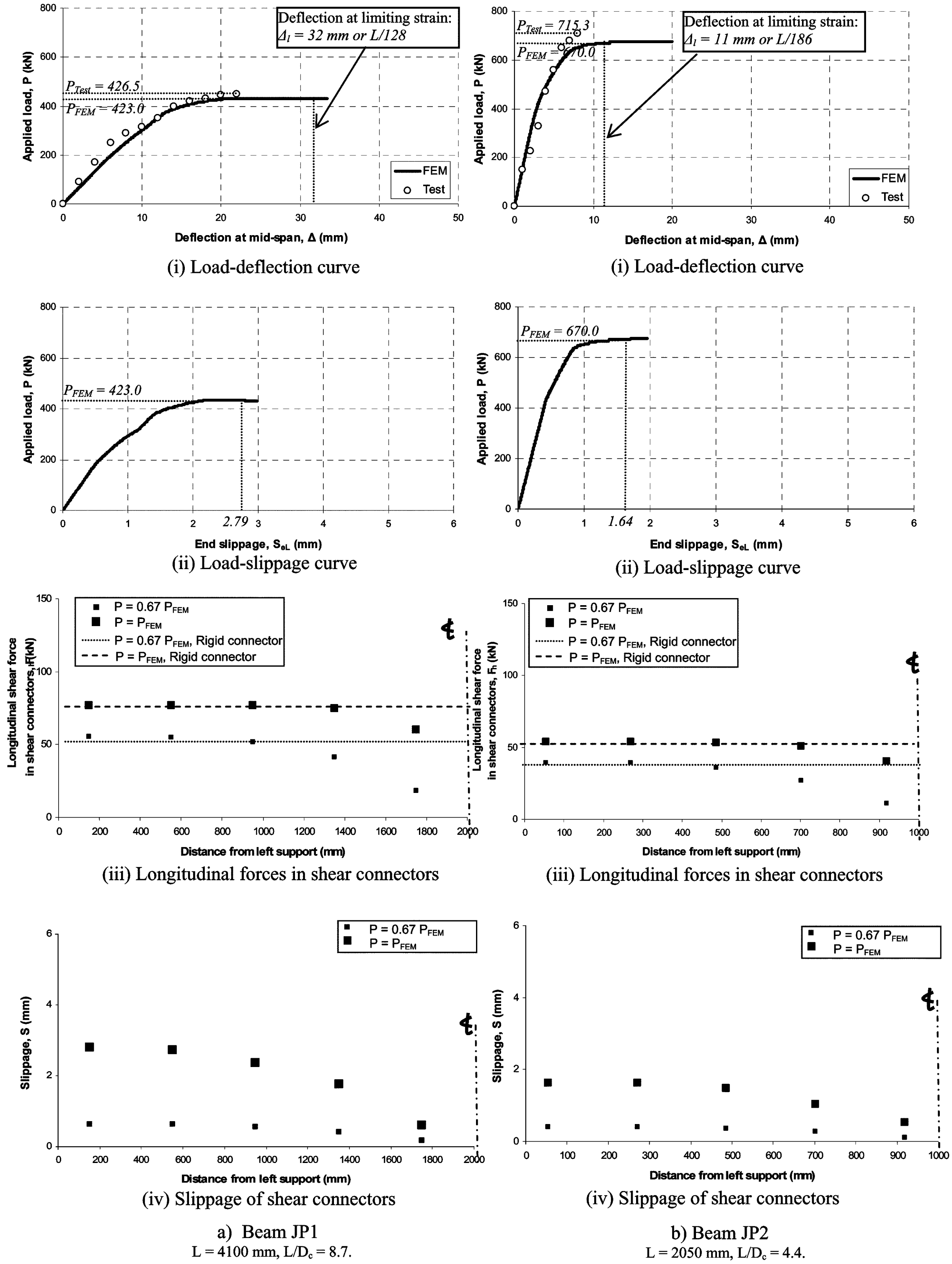

Fig. 9 Numerical results of Beams JP1 and JP2

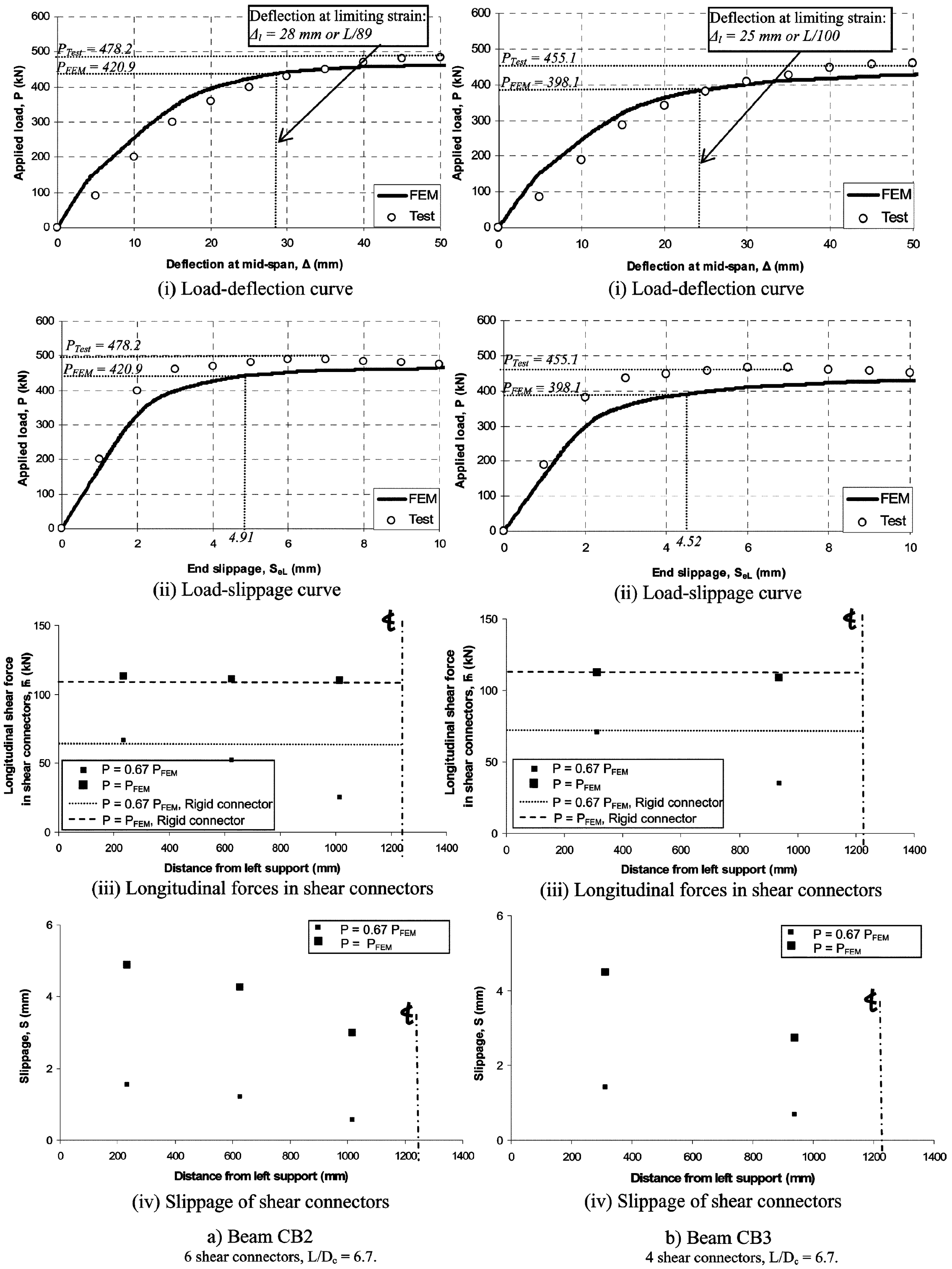

Fig. 10 Numerical results of Beams CB2 and CB3

Table 3 Ultimate loads of composite beams

Beam test	Degree of shear connection at mid-span	Shear force ratio at failure	Mode of failure	Measured load from test, P_{Test} (kN)	Predicted load from model, P_{FEM} (kN)	P_{Test}/P_{FEM}
B2	0.67	0.40	Flexural	301.3	303.1	0.99
B4	0.47	0.39	Flexural	283.3	279.7	1.01
JP1	0.32	0.62	Flexural	426.5	423.0	1.01
JP2	0.24	0.72	Flexural and Shear	715.3	670.0	1.07
CB2	0.17	0.47	Flexural	478.2	420.9	1.14
CB3	0.12	0.43	Flexural	455.1	398.1	1.14

4.3. Cross-sectional distributions of stresses and strains

The cross-sectional deformation characteristics of the composite beams at failure obtained from the finite element models are presented in Fig. 11 where both the longitudinal direct strains and stresses of the concrete slabs and the steel beams of all the six composite beams are plotted on the same graph with the same scales for direct comparison.

For composite beams with modest span over depth ratios, namely Tests B2 and B3, the variations of both the strains and the stresses are found to be linear within the respective depths of the concrete slabs and the steel beams despite of the presence of discontinuity at the interface between the concrete slabs and the steel beams due to the slippages of shear connectors. For short span composite beams, namely, Tests JP1, JP2, CB2 and CB3, significant non-linearity in both the strains and the stresses are apparent within the depths of the steel beams, as expected, due to the effect of high shear forces. Hence, it is shown that the models are capable of predicting accurately the cross-sectional deformation characteristics of composite beams with a wide range of practical parameters.

4.4. Flexible shear connectors

In order to understand the roles of flexible shear connectors in all these six composite beams, the distributions of longitudinal shear forces in shear connectors along the beam spans at both elastic and ultimate stages are examined. It is shown in Figs. 8, 9 and 10 that due to the flexibility of shear connectors, slippages between the concrete slabs and the steel beams are required to take place in order to mobilize the shear resistances of the shear connectors, particularly for those shear connectors near the supports. For all composite beams under sagging moments, namely, Tests B2, B4, JP1 and JP2, with degrees of shear connection ranging from 0.67 to 0.24, the predicted shear resistance distributions are found to follow those obtained from structural mechanics, i.e., uniform over shear spans between point loads. Moreover, for composite beams under hogging moments, namely, Tests CB2 and CB3, with degrees of shear connection below 0.2, the predicted shear resistance of the shear connectors are also shown to be uniform, and they are readily mobilized in the way similar to those shear connectors in composite beams under sagging moments. However, it should be noted that in general, these shear connections are required to deform significantly, with a slippage of 6 to 8 mm, in order to mobilize the hogging moment resistances of the composite sections.

Consequently, it is shown that the shear resistances of the shear connectors in composite beams with long to short spans under both sagging and hogging moments are readily mobilized, irrespective of the

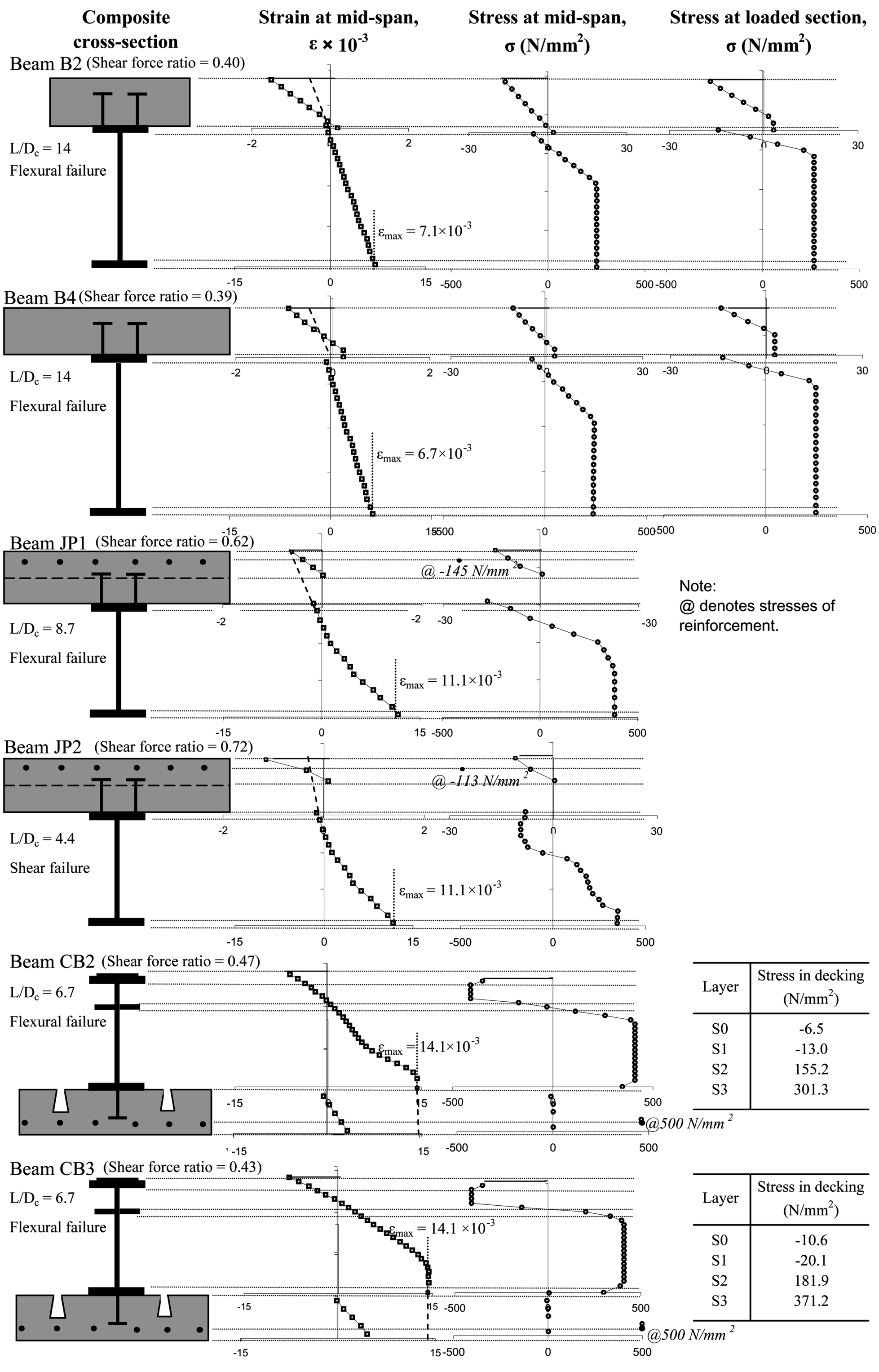

Layer	Stress in decking (N/mm²)
S0	-6.5
S1	-13.0
S2	155.2
S3	301.3

Layer	Stress in decking (N/mm²)
S0	-10.6
S1	-20.1
S2	181.9
S3	371.2

Fig. 11 Distributions of stresses and strains at critical cross sections

degrees of shear connection of the composite beams. However, it is necessary to use shear connectors with large ductility against slippage to ensure that all the composite beams are able to sustain the maximum applied loads at large deformation. Separate investigation into the structural behaviour of composite beams will be needed if non-ductile shear connectors are used instead, and this will be easily achieved by modifying the load-slippage curves of the shear connectors in the finite element models.

It should be noted in Fig. 8 that the measured slippages of the shear connectors are significantly larger than those predicted values by typically 0.8 to 1.0 mm or 25 to 30% in both Beams B2 and B4. The discrepancy may arise from the fact that the deformation characteristics of shear connections in the push-out tests is fundamentally different to those in the beam tests, and further investigation into representative deformation characteristic of shear connectors in composite beams should be carried out as appropriate.

5. Conclusions

This paper presents the development study as well as the calibration exercise of the proposed finite element models for simply supported composite beams. A total of six composite beams with detailed test results are selected from the literature, and finite element models of these beams are established to study their structural performance.

Due to the high efficiency of the proposed finite element models, the computational efforts of these models are found to be minimal. Numerical results such as load mid-span deflection curves and load end-slippage curves are fully presented, and comparison with test data is made whenever available. It is shown that the finite element models are able to predict the deformation characteristics of the composite beams satisfactorily during the entire deformation ranges. Other structural deformation characteristics of the composite beams such as cross-sectional distributions of stress and strain, and distributions of shear forces and slippages in shear connectors along beam spans are also presented.

It should be noted that as no local buckling is incorporated into the proposed models, the models are only applicable to composite beams with I sections classified as at least compact sections. Also refer to Tables 1 and 2 for the ranges of applicability of various geometrical dimensions and material properties of the composite beams.

The proposed models are readily extended to cover various practical design cases as follows:

- steel and composite beams with fabricated asymmetric I sections, and fabricated I sections with tapered webs,
- steel and composite beams with single and multiple web openings of different sizes and shapes, as well as eccentric and reinforced web openings,
- composite beams and floor systems with web openings for passage of building services,
- composite beams with partial continuity offered by the connections to columns, and
- both unprotected and protected composite beams under fires.

Structural engineers are strongly encouraged to employ the models in their practical work to exploit the full advantages offered by composite construction.

Acknowledgements

The project leading to the publication of this paper is supported by the Research Committee of the Hong Kong Polytechnic University (Project No. G-W039).

References

ABAQUS. (2004). User's Manual, Version 6.4, Hibbitt, Karlsson and Sorensen, Inc.

Australian Institute of Steel Construction and Standards Australia. (1997), Composite beam design handbook in accordance with AS2327.1 - 1996, SAA HB91.

Baskar, K., Shanmugam, N. E. and Thevendran, V. (2002), "Finite-element analysis of steel-concrete composite plate girder", *J. Struct. Eng.,* **128**(9), 1158-1168.

British Standards Institution (1990), BS5950: Structural use of steelwork in building. Part 3 Section 3.1: Code of practice for design of composite beams.

British Standards Institution. prEN 1994-1-1. (2002), Eurocode 4: Design of composite steel and concrete structures. Part 1.1: General rules and rules for buildings. European Committee for Standardization.

Cas, B., Bratina, S., Saje, M. and Planinc, I. (2004), "Non-linear analysis of composite steel-concrete beams with incomplete interaction", *Steel Compos. Struct.*, **4**(6), 489-507.

Chung, K. F. and Wang, A. J. (2004), "Verification to design of perforated composite beams using finite element method", *Proc. Int. Conf. Steel and Composite Structures*, Seoul, Korea, 2 - 4 September 2004 (CD publication).

Chung, K. F., Ko, C. H. and Wang, A. J. (2005), "Design of steel and composite beams with web openings – Verification using finite element method", *Steel Compos. Struct.*, **5**(2-3), 203-234.

Fang, L. X., Chan, S. L. and Wong, Y. L. (2000), "Numerical analysis of composite frames with partial shear-stud interaction by one element per member", *Eng. Struct.* **22**(10), 1285-1300.

Gattesco, N. (1999), "Analytical modelling of nonlinear behaviour of composite beams with deformable connection", *J. Const. Steel Res.*, **52**, 195-218.

Hassan, A. F. M. and Mourad, S. A. (2002), "Numerical modeling of composite beams with web openings", *J. Engineering and Applied Science*, **49**(1), 89-107.

Jayas, B. S. and Hosain, M. U. (1989), "Behaviour of headed studs in composite beams: Full size tests", *J. Civil Eng.,* **16**, 712-724.

Johnson, R. P. and Anderson, D. (2001), Designers' Handbook to Eurocode 4: Part 1.1: Design of composite steel and concrete structures. Thomas Telford, London.

Lam, D. and El-Lobody, E. (2005), "Behavior of headed stud shear connectors in composite beam", *J. Struct. Eng.,* **131**(1), 96-107.

Lawson, R. M. (1989), Design of composite slabs and beams with steel decking. The Steel Construction Institute.

Lawson, R. M. and Chung, K. F. (1994), Composite beam design to Eurocode 4. The Steel Construction Institute.

Loh, H. Y., Uy, B. and Bradford, M. A. (2004a), "The effects of partial shear connection in the hogging moment regions of composite beams, Part I – Experimental study", *J. Const. Steel Res.,* **60**(6), 897-919.

Loh, H. Y., Uy, B. and Brandford, M. A. (2004b), "The effects of partial shear connection in the hogging moment regions of composite beams, Part II – Analytical study", *J. Const. Steel Res.,* **60**(6), 921-962.

McGarraugh, J. B. and Baldwin, J. W. (1971), "Lightweight concrete-on-steel composite beams", *Eng., J.* **8**(3), 90-98.

Oehlers, D. J. and Bradford, M. A. (1995), *Composite Steel and Concrete Structural Members: Fundamental Behaviour.* Pergamon.

Oehlers, D. J. and Sved. G. (1995), "Composite beams with limited-slip-capacity shear connectors", *J. Struct. Eng.,* **121**(6), 932-938.

Standards Australia, Australian Standard AS2327.1. (1996), Composite Structures. Part 1: Simply supported beams. Standards Australia International Ltd.

The Buildings Department of the Government of Hong Kong SAR. (2005), The Hong Kong Steel Code: Chapter 10 Composite Structures.

Wang, Y. C. (1998), "Deflection of steel-concrete composite beams with partial shear interaction", *J. Struct. Eng.,* **124**(10), 1159-1165.

BU